Charge-Reversal Instability in Mixed Bilayer Vesicles

Yi Chen and Philip Nelson
Department of Physics and Astronomy, University of Pennsylvania, Philadelphia PA 19104
(16 February 2000)

Abstract

Bilayer vesicles form readily from mixtures of charged and neutral surfactants. When such a mixed vesicle binds an oppositely-charged object, its membrane partially demixes: the adhesion zone recruits more charged surfactants from the rest of the membrane. Given an unlimited supply of adhering objects one might expect the vesicle to remain attractive until it was completely covered. Contrary to this expectation, we show that a vesicle can instead exhibit *adhesion saturation,* partitioning spontaneously into an attractive zone with definite area fraction, and a repulsive zone. The latter zone rejects additional incoming objects because counterions on the interior of the vesicle migrate there, effectively reversing the membrane's charge. The effect is strongest at high surface charge densities, low ionic strength, and with thin, impermeable membranes. Adhesion saturation in such a situation has recently been observed experimentally [H. Aranda-Espinoza *et al.*, *Science* **285** 394–397 (1999)].

82.65.Dp, 82.65.Fr, 82.70.Dd, 87.10.+e, 87.15.Kg, 87.16.Dg

I. INTRODUCTION

The self-assembly of colloidal particles offers an attractive route to the synthesis of highly ordered, nanostructured materials. Typically these materials have been extremely soft, being stabilized by entropic effects.

For example, classical colloidal crystals are three-dimensional arrays of mutually repelling spheres [1,2]. Entropic effects maintain their crystalline order in spite of a density well below that of close-packing. As a result, these arrays are easily disrupted by small mechanical shear, dilution, *etc.* More recently, depletion forces have been harnessed to assemble spheres into crystalline arrays on the walls of their container [3]. Again the physical forces between the spheres are repulsive, and again the resulting arrays are extremely soft.

Attempts to create strong ordered materials from physically *attracting* components have generally produced instead highly disordered aggregates. Recently, however, Ramos *et al.* reported the observation of robust two-dimensional crystallites formed from negatively-charged latex spheres introduced into a suspension of bilayer vesicles [4,5]. The membranes forming the vesicles consist of a mixture of positively-charged and neutral surfactants. The immense electrostatic attraction between the negative spheres and positive membranes led to the crystallites' great strength; their ordered 2d character arose *via* the intermediary role of the vesicles as *templates* for the initial self-assembly of the spheres.

In this paper we develop some of the physics of the crucial intermediate step just mentioned, elaborating and extending the discussion in [4]. This stage begins when the latex spheres are first introduced to the vesicle suspension, and lasts for hours to days. Initially the spheres adsorb avidly onto the vesicles, and indeed many vesicles become completely covered with spheres. However, a significant subpopulation of vesicles content themselves with only partial coverage: on these vesicles the adsorbed spheres form a *self-limiting 'raft'*. Once the raft forms, no further spheres attach to the vesicle anywhere, though they are present in excess. Instead, particles in suspension are seen to approach, then wander away from, the vesicle.

The theory of colloidal surface interactions is vast (for introductions see [6–8]). Our goal is to introduce a very simple mechanism for adhesion saturation, summarized graphically in Fig. 1 below, then present some calculations to show how it works in the parameter regime relevant to experiments. We will argue that our effect should be qualitatively unchanged after many other surface-interaction effects are included in the analysis, but much work remains to be done to show this in detail. Sect. II sketches the physics of our mechanism. Sect. III begins the analysis using linearized Poisson–Boltzmann theory, considering in turn a series of more complicated situations. The linearized theory is familiar and helps to connect the analysis to the physical picture, but it proves to be inadequate for the interesting range of parameter values. Thus in Sect. IV we upgrade to the full nonlinear theory, which proves to be quite easy in this context. Finally we consider the effects of ion correlations, neglected in Poisson–Boltzmann theory, in Sect. V. A glossary of symbols appears in the Appendix.

II. PHYSICAL PICTURE

We first briefly review the physical picture developed in [4] and summarized in Fig. 1.

Consider first two dielectric surfaces bearing fixed charge densities $\sigma_\pm$ of the same magnitude but opposite sign in an electrolyte solution. When they are separated by several screening lengths they feel little mutual attraction, since each maintains a neutralizing cloud of counterions. As the surfaces approach closer, eventually their screening clouds begin to interpenetrate. Then negative counterions from the positive surface, and positive counterions from the negative surface, can escape to infinity without violating overall charge neutrality. The corresponding gain in entropy reduces the system's free energy: counterion release drives the surfaces into contact.

Next consider the case of two surfaces of opposite sign and *unequal* magnitude; for instance, suppose that $\sigma_+ < |\sigma_-|$. In this case counterion release will be incomplete; after exhausting all the negative counterions, some positive ones will remain, trapped by the requirement of charge neutrality. The osmotic pressure of the trapped ions will prevent the surfaces from coming into perfect contact. If one surface has *variable* charge density, say σ_+, then additional surface charges will be pulled into the contact region in order to improve the contact with the approaching negative surface [9]. A surface charge density can for instance vary because the *composition* of the surface is variable: for instance, the surface may be a mixture of charged and neutral surfactants, as in the experiments of [4,5]. In this case the recruitment of charge to the contact region will deplete the other regions, in turn rendering them less attractive to additional negative dielectric objects. Fig. 1*c* depicts this situation: surfactant rearrangement in the outer monolayer of the membrane has permitted the release of two more ion pairs than would otherwise (panel *b*) have been possible.

The rearrangement of membrane charges is limited: the relative concentration of charged surfactants cannot exceed unity. The maximum charge density on the outer monolayer may still be less than that of the approaching dielectric, and so the final contact may still be imperfect, as shown in Fig. 1*c*. We will assume this to be the case in the rest of this paper.

Nevertheless, a further reduction in free energy density from Fig. 1*c* is still possible, once we remember that the inner membrane monolayer and its counterions need not play a passive role. Fig. 1*d* shows how the remaining trapped counterions in panel *c* can leave the gap, even if the membrane is impermeable, by following the dashed horizontal arrows in panel *c*. After this rearrangement some of the charge on the negative dielectric is neutralized by surfactants on the inner monolayer, whose own interior counterions migrate to the nonadhesion region.[1] Panel *c* also shows a rearrangement of the surfactants on the *inner* monolayer, further depleting the charge of the noncontact zone.

Fig. 1*d* raises an intriguing question: will the migration of interior counterions ever overwhelm and effectively reverse the charge of the membrane as seen from outside, as shown in the figure? Of course, cartoons alone will not settle this question, but we can argue physically that such an effect may well happen as follows. First we note that the

[1]Even if the dielectric's charge exceeds twice the monolayer charge density, as assumed in the text below, additional $\pm$ ion pairs can be brought from the membrane interior, with the positive ions remaining in the adhesion region to help neutralize the dielectric and the negative ones migrating to the nonadhesion region, driving its net charge still more negative.

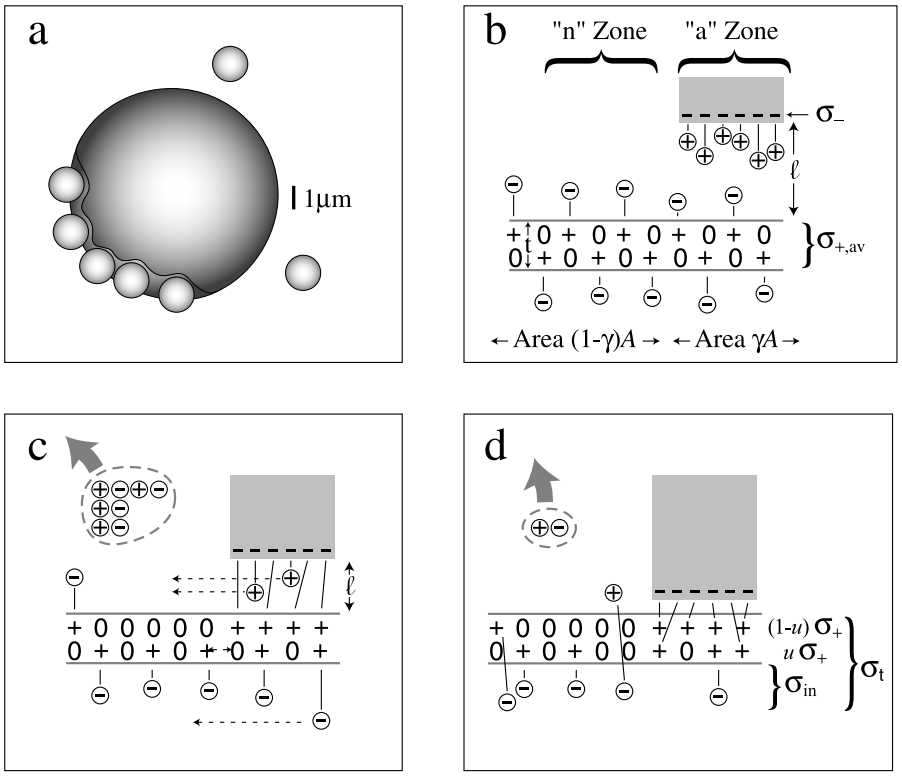

FIG. 1. *(a)* Cartoon of the situation. A large vesicle of mixed neutral and positively-charged surfactants attracts a limited number of negatively-charged spheres, then saturates. The Debye screening length, typically about 10 nm, is much smaller than the sizes of the objects.

(b) Disposition of counterions when an approaching negative object (shaded, above right) is still far from the vesicle. The vesicle interior is at the bottom of the figure. The zeros denote neutral surfactants, plus signs the charged surfactants. Circled ± signs denote counterions in solution. The solid vertical lines joining charges are fictitious elastic tethers representing intuitively the electric field lines; the requirement of charge neutrality translates visually into the requirement that all charges be tied in this way.

(c) Redistribution of charges when the negative dielectric object approaches the membrane, if we artificially forbid any electric field inside the membrane. Four pairs of counterions have been released to infinity (upper left). The interior monolayer, and its counterion cloud, are unchanged from *(b)*. Zone "n" presents a net of one positive charge to the vesicle exterior and so remains attractive to further incoming negative objects.

(d) The resulting state after we relax the constraint of zero electric field inside the membrane, allowing the ion migrations indicated by the horizontal dashed arrows in *(c)*. One additional counterion pair has been released to infinity and the adhesion gap has narrowed. The net charge of the bilayer plus interior counterions in zone "n" has reversed sign relative to *(c)*, and so this zone repels additional incoming negative objects. [Adapted with permission from [4]. © 1999 American Association for the Advancement of Science.]

positive charge density of the noncontact zone "n" is already very small in Fig. 1*c*, since the interior monolayer and its counterion cloud cancel, and as we will see below the electrostatic interaction driving the depletion of charged surfactants from the outer monolayer is very strong. Thus only a small migration of interior counterions will suffice to get charge reversal. Second, the entropic *cost* of creating a nonuniform charge density in the interior counterion cloud is quadratic in the amount of charge which migrates, since the uniform distribution is an equilibrium state. But the free energy *gain* from this redistribution is linear in the amount of charge migration, being dominated by the derivative $\mathrm{d}/\mathrm{d}\sigma_+$ of the attractive self-energy (see formula (3.9) below). Thus a finite amount of counterion migration will occur, and this amount may well exceed the small net charge on the nonadhesion region, effectively reversing it.

The rest of this paper is devoted to a quantitative justification of the intuitive argument just given. Before passing on to the analysis, we should remark on another feature of Fig. 1*d*. Charge reversal requires that electric fields (represented schematically by the vertical lines in the figure) penetrate the interior of the membrane. Since the membrane interior is a low dielectric constant medium, the energetic cost of these fields can be significant, another term quadratic in the amount of charge migration from panel *c* to *d*. If the membrane is sufficiently thick, this cost will reduce the charge migration below the point of charge reversal, a point we will need to examine quantitatively in Sect. IV C below.

III. LINEARIZED MEAN-FIELD THEORY

In this section we begin the mathematical implementation of the ideas in Sect. II. We begin with the linearized (Debye-Hückel) limit of low charge density, even though ultimately we will argue that the experiments studied here require a full nonlinear treatment. We do this partly because of the simplicity of the formulæ, and partly to make contact with earlier work.

To fix notation and keep the article self-contained we begin by rederiving some key results from [10,11,9]. The Appendix summarizes our units and all symbols used throughout the paper.

A. Basic formulæ

The electrostatic potential energy of a distribution of free charges of density $\rho(\mathbf{r})$ is $\frac{1}{2}\int \mathrm{d}\mathbf{r}\,\rho(\mathbf{r})\psi(\mathbf{r})$, where ψ is the electric potential [12]. The potential created by a single point charge q in an infinite, uniform, dielectric medium is $\psi(\mathbf{r}) = q/4\pi\epsilon|\mathbf{r}|$. In a more complicated situation, $\psi(\mathbf{r})$ is related to $\rho(\mathbf{r}')$ by some Green function $G(\mathbf{r},\mathbf{r}')$ and obeys Poisson's equation, $\nabla^2\psi = -\rho/\epsilon$.

We first imagine a uniform charge distribution of density σ on the surface $\{z=0\}$.[2] The halfspace $z<0$ is filled with a dielectric with no free charges, and so the electric field must

[2]The assumption of fixed charge is appropriate for surfaces with fully-ionized groups at the pH

everywhere vanish here. The other halfspace is a univalent salt solution in equilibrium with a reservoir at concentration $\hat{n}$. The reservoir must remain neutral, but it can supply ion pairs at a cost in free energy given by a chemical potential $\mu k_{\rm B}T$. The total free energy of the mobile ions near the surface is then $F = F_{\rm ent} + F_{\rm es}$, where the entropic and electrostatic energies in mean-field approximation are [8]

$$F_{\rm ent} = k_{\rm B}T \int {\rm d}\mathbf{r}\ [n_+(\ln n_+ v_0 - 1) + n_-(\ln n_- v_0 - 1) - \mu(n_+ + n_-) + \xi(n_+ - n_- + n_{\rm f})] \tag{3.1}$$

$$F_{\rm es} = \tfrac{1}{2} \int {\rm d}\mathbf{r}{\rm d}\mathbf{r}'\, e n_{\rm tot}(\mathbf{r}) G(\mathbf{r},\mathbf{r}') e n_{\rm tot}(\mathbf{r}') \ . \tag{3.2}$$

In the above formulæ, $n_\pm$ are the number densities of ions, while $n_{\rm tot}(\mathbf{r}) = \rho/e = n_+ - n_- + n_{\rm f}$ is the total signed density, including fixed surface charges with signed density $n_{\rm f}$. We introduced a Lagrange multiplier ξ to enforce overall neutrality. The symbol v_0 is a microscopic volume factor which will drop out of all physical results. We have fixed the arbitrary constant in $F_{\rm es}$ by setting the electrostatic energy to zero when the mobile counterions form a sheet coinciding with the fixed surface charge. Thus $F_{\rm es}$ is the work needed to pull this sheet away from the surface, and so is a positive quantity.

In equilibrium we have $\frac{\delta F}{\delta n_\pm(\mathbf{r})} = 0$. Away from the plane this fixes

$$n_\pm(\mathbf{r}) v_0 = {\rm e}^{\mu \mp (\bar{\psi}(\mathbf{r}) + \xi)} \ , \quad z > 0 \ . \tag{3.3}$$

Here $\bar{\psi} = e\psi/k_{\rm B}T$ and we have fixed the additive constant in ψ by choosing $\psi(\infty) = 0$. Since $n_+ = n_- = \hat{n}$ at infinity, we get $\xi = 0$ and $\mu = \ln \hat{n} v_0$, or

$$n_\pm(\mathbf{r}) = \hat{n} {\rm e}^{\mp \bar{\psi}(\mathbf{r})} \ . \tag{3.4}$$

Substituting then gives the free energy

$$F = k_{\rm B}T\hat{n} \int {\rm d}\mathbf{r}\ \left[\bar{\psi}\sinh\bar{\psi} - 2\cosh\bar{\psi} + \tfrac{1}{2}(n_{\rm f}/\hat{n})\bar{\psi} + 2\right] \ . \tag{3.5}$$

The last term of (3.5) is a constant which we have added by hand to cancel a term proportional to the volume of the world.

Eqn. (3.5) simplifies if the dimensionless potential $\bar{\psi}$ is everywhere $\ll 1$; in this case we simply get $F = k_{\rm B}T \int {\rm d}\mathbf{r}\, \frac{1}{2} n_{\rm f} \bar{\psi}$. Since the fixed charge n_f is confined to a plane, the free energy is a purely surface term once $\bar{\psi}$ has been found.

To find $\bar{\psi}$, we note that it satisfies the Poisson equation, a property of the Green function used to define it. Using the charge density $e n_\pm(\mathbf{r})$ found above in (3.4) gives the Poisson-Boltzmann equation,

---

used, such as those in the experiments of [4,5]. We also implicitly assume that the surfactants used are insoluble in water, so that their numbers in the membrane are fixed. This assumption may need further scrutiny, since in the experiments one surfactant species forms micelles.

$$\nabla^2\bar{\psi} = \frac{2e^2\hat{n}}{\epsilon k_{\rm B}T}\sinh\bar{\psi}\ . \tag{3.6}$$

Linearizing then gives the familiar Debye-Hückel equation: $\nabla^2\bar{\psi} = \kappa^2\bar{\psi}$, where $\kappa = \sqrt{2e^2\hat{n}/\epsilon k_{\rm B}T}$.

The objects we want to consider are much bigger than the screening length $\lambda_D = 1/\kappa$ (see Fig. 1a). Thus our geometry is essentially planar, and we need the planar solutions $\bar{\psi}(z) = B{\rm e}^{\pm\kappa z}$ to the Debye-Huckel equation. The electric field is then $\mathbf{E} = -\boldsymbol{\nabla}\psi$, which indeed decays exponentially on the length scale λ_D.

For a single wall we must choose the decaying solution to (3.6). We fix the constant B by imposing Gauss's law at the surface: $\mathbf{E} = -\frac{\partial\psi}{\partial z}\hat{\mathbf{z}} = \frac{\sigma}{\epsilon}\hat{\mathbf{z}}$. Then $B = \sigma e/\kappa\epsilon k_{\rm B}T$, the solution is

$$\bar{\psi}(z) = \frac{\sigma e}{\kappa\epsilon k_{\rm B}T}{\rm e}^{-\kappa z}\ . \qquad \text{(linearized approximation)} \tag{3.7}$$

and the free energy per unit area of the isolated, charged surface is

$$f_{\rm self} \equiv F/(\text{area}) = k_{\rm B}T\sigma B/2e = \sigma^2/2\kappa\epsilon\ . \qquad \text{(linearized approximation)} \tag{3.8}$$

Another well-known solution to (3.6) arises in the opposite case of very high charge density, where $\bar{\psi} \gg 1$ at the surface. In this case the Poisson-Boltzmann equation has a solution of "Gouy-Chapman" form: $\bar{\psi}(z) = \ln\left[\frac{2\epsilon k_{\rm B}T}{e^2\hat{n}}\frac{1}{(z+\lambda_{\rm GC})^2}\right]$. Here the free parameter is the offset $\lambda_{\rm GC}$, chosen to enforce Gauss's law: $\lambda_{\rm GC} = 2\epsilon k_{\rm B}T/e\sigma$. More highly-charged surfaces thus have smaller $\lambda_{\rm GC}$ and so a more nearly singular potential. The pathological behavior of $\bar{\psi}$ at large z simply reflects the end of the regime $\bar{\psi} \gg 1$ at large enough z. Note that the electric field $E_z = 2k_{\rm B}T/e(z+\lambda_{\rm GC})$ of the Gouy-Chapman solution is independent of the ambient salt concentration $\hat{n}$, as it should be: the electric forces near a highly charged surface depend only on the surface charge. The salt concentration determines only the extent of the region in which the strong-field approximation is valid.

B. Two dielectrics

We minimized the free energy of an isolated surface, obtaining (3.8). To extract any useful work from this stored free energy, we would have to remove some constraint. One way to do this is to bring in another semiinfinite, planar dielectric[3] bearing opposite surface

[3]Nothing is really infinite. The phrase "semiinfinite planar dielectric" will mean a finite dielectric object whose surface curvature is much smaller than κ, whose interior contains no free charges, and whose volume is large enough that any interior electric field would be prohibitively expensive in energy. As two such objects approach, the gap ℓ between them decreases but the total volume occupied by solution doesn't change; this is why the constant we subtracted from (3.5) really is a constant.

charge, thus changing the solution region from a half-space to a planar slab of thickness ℓ. Let us suppose that a surface with $\sigma_+ > 0$ approaches another surface with $\sigma_- < 0$.

Parsegian and Gingell studied this situation in the linearized approximation [10], arguing as in Sect. II that the surfaces attract *via* counterion release until all of one species of counterions in the gap (the "minority" species) has been exhausted. If $\sigma_+ \neq |\sigma_-|$, a residual cloud of the other ("majority") species remains in the gap and the system equilibrates at a finite gap spacing ℓ_*. Nevertheless, the final state has less free energy per unit area than it did originally; the difference is the *adhesion strength* W.

We could compute W by again solving a boundary-value problem as in Sect. III A, but there is a shortcut. Suppose that $\sigma_+ < |\sigma_-|$, so that the + counterions are the "majority" species. In mechanical equilibrium the hydrostatic pressure pushing the walls together vanishes. The planar Poisson-Boltzmann equation is a second-order ordinary differential equation, and so its solutions form a two-parameter family. One integration constant is fixed by the Gauss-law boundary condition on the negative wall, while in equilibrium the other is fixed by the condition of vanishing pressure. Hence the solution $\bar{\psi}(z)$ is exactly the same for two walls as it is for the isolated negative wall; the only difference is that in the former case we truncate the solution at $z = \ell_*$, while in the latter case z extends to infinity. The equilibrium gap spacing ℓ_* is then just the value of z at which Gauss's law for the positive wall is satisfied: $-(-\frac{\partial\psi}{\partial z}) = \frac{\sigma_+}{\epsilon}$. Then (3.7) gives the equilibrium spacing ℓ_* by $\mathrm{e}^{\kappa\ell_*} = |\sigma_-/\sigma_+|$ in the linearized approximation. Note that indeed the right side of this formula is positive and greater than unity, as it must be since $\ell_* \geq 0$.

We now recall that the linearized approximation retains only the boundary term of (3.5), so

$$\begin{aligned} f_{\mathrm{gap}}(\sigma_+, \sigma_-) &= \frac{k_{\mathrm{B}}T}{2e}\left[\sigma_-\bar{\psi}(0) + \sigma_+\bar{\psi}(\ell_*)\right] \\ &= \frac{1}{2\kappa\epsilon}((\sigma_-)^2 - (\sigma_+)^2) \ . \end{aligned} \tag{3.9}$$

Repeating these steps for the opposite case where $\sigma_+ > |\sigma_-|$, we find that in general (Fig. 2*a*)

$$f_{\mathrm{gap}}(\sigma_+, \sigma_-) = |f_{\mathrm{self}}(\sigma_+) - f_{\mathrm{self}}(\sigma_-)| \ . \tag{3.10}$$

Remarkably, the simple combination formula (3.10) will continue to hold in the full nonlinear Poisson-Boltzmann treatment of Sect. IV A below.[4] Formula (3.10) is certainly reasonable: when $\sigma_+ = |\sigma_-|$ all counterions get released, the two surfaces coincide, and this was our reference state of zero energy. Also, when we reverse the signs of all the charges the free energy should not change; (3.10) has this property.

Finally we find the adhesion energy W as [9]

$$W = f_{\mathrm{self}}(\sigma_+) + f_{\mathrm{self}}(\sigma_-) - f_{\mathrm{gap}}(\sigma_+, \sigma_-) = \min\{(\sigma_+)^2, (\sigma_-)^2\}/\epsilon\kappa. \text{ (linearized approximation)} \tag{3.11}$$

[4]Behrens and Borkovec have independently used this fact to simplify the study of nonlinear PB solutions [13].

Note that W is completely independent of the majority charge density, a property noted by Nardi *et al.* In light of the physical picture in Sect. II, we can readily interpret that fact: The total counterion release is limited by the *smaller* of the two counterion populations.

Since W is always positive we find, as expected, that *oppositely-charged dielectrics always attract* via the counterion-release mechanism [10]. Of course this is not the behavior we were seeking to explain (see Sect. I). We must now proceed to generalize the above arguments, incorporating the relevant differences between the above system and the one studied in the experiments of [5].

C. Thick membrane

We just found that two oppositely-charged dielectrics attract, as expected. But the experiments we are studying involve dielectric (latex) spheres interacting not with other dielectrics, but with a bilayer *membrane*. In this subsection we begin to incorporate the new physics associated with this situation. We first study the interaction of a dielectric of fixed charge density $\sigma_- < 0$ with a positively-charged, very thick, membrane, recapitulating some results of Nardi *et al.* [9].

The new physical feature of this situation is that the bilayer membranes in the experiments are *fluid mixtures* of positively-charged and neutral surfactants. This means that the charge density σ_+ on the membrane is not a fixed number, but may vary subject to $\sigma_+ > 0$ and the overall constraint that the total membrane charge $\int \mathrm{d}A\, \sigma_+$ is fixed. Let $\sigma_{+,\mathrm{av}}$ denote the average charge density, so that the total membrane charge is $A\sigma_{+,\mathrm{av}}$. In addition we will suppose that the charge density cannot exceed a maximum of $\sigma_{\max} = 2e/a_0$ determined by the area per headgroup a_0 of the charged surfactants in each of the two monolayers constituting the membrane, and that $|\sigma_-| > \sigma_{\max}$.

Throughout this paper we will adopt a highly simplified, generic picture of membrane compositional changes, retaining only the entropy of mixing of the two surfactant types. Thus we neglect other entropic or enthalpic packing effects in the assumed membrane free energy f_{m}. Moreover, at first we will for simplicity neglect the bilayer structure of the membrane; later on we will use formulæ appropriate to a bilayer. With these simplifications f_{m} takes the form

$$f_{\mathrm{m}} = \frac{2}{a_0} k_{\mathrm{B}} T \left[\frac{\sigma_+}{\sigma_{\max}} \ln \frac{\sigma_+}{\sigma_{\max}} + \Big(1 - \frac{\sigma_+}{\sigma_{\max}}\Big) \ln\Big(1 - \frac{\sigma_+}{\sigma_{\max}}\Big) \right] . \tag{3.12}$$

As discussed in Sect. II, we wish to explore the possibility of a spontaneous partition of the membrane into two uniform regions, which we will call zones "a" and "n". (Ultimately we hope to find that "a" is *a*dhering while "n" is *n*onadhering, but for the moment these are arbitrary names.) The areas of the two zones are not known in advance, but they must add up to the total area A, so we take them to be γA and $(1-\gamma)A$ respectively.

The two zones exchange one conserved quantity, namely membrane charge.[5] Thus the

[5] A second conserved quantity, the total charge of the counterions, is not independent but instead fixed by charge neutrality.

system can divide into zones of charge density $\sigma_+^{(a)}$ and $\sigma_+^{(n)}$, subject to

$$\gamma\sigma_+^{(a)} + (1-\gamma)\sigma_+^{(n)} = \sigma_{+,\mathrm{av}} \ . \tag{3.13}$$

This separation will be energetically advantageous if the corresponding total free energy $A(\gamma f(\sigma_+^{(a)}) + (1-\gamma)f(\sigma_+^{(n)}))$ is less than $Af(\sigma_{+,\mathrm{av}})$. Here the free energy density $f(\sigma_+)$ is computed for a *uniform* zone with fixed membrane charge density σ_+, minimizing over all other variables.

The instability just described will not occur if $f(\sigma_+)$ is a convex function, i.e. $\mathrm{d}^2 f/\mathrm{d}{\sigma_+}^2 > 0$. If $\mathrm{d}^2 f/\mathrm{d}{\sigma_+}^2$ is negative anywhere within the allowed region $0 < \sigma_+ < \sigma_{\mathrm{max}}$, we apply the Maxwell construction from thermodynamics to the graph of f. This involves drawing a straight line tangent to the graph and spanning the region of concavity. Let the two points of tangency be located at $\sigma_+^{(a)}$ and $\sigma_+^{(n)}$. If the average membrane composition $\sigma_{+,\mathrm{av}}$ lies between these two values, then the uniform system will be unstable to partitioning into two zones with compositions $\sigma_+^{(a)}$ and $\sigma_+^{(n)}$.

In the case of a thick membrane, we have $f = f_{\mathrm{gap}}(\sigma_+) + f_{\mathrm{m}}(\sigma_+)$. Consulting (3.10), (3.8), and (3.12), we find that the first (electrostatic) term is destabilizing, while the second (entropic) term is stabilizing. For future use we introduce two convenient abbreviations, one parameterizing the relative strengths of the two terms, the other a dimensionless measure of charge density:

$$\beta \equiv 2\hat{n}a_0/\kappa = \kappa a_0/4\pi\ell_B \ , \qquad \bar{\sigma} \equiv \sigma/\sigma_{\mathrm{max}} \ . \tag{3.14}$$

With these abbreviations we obtain

$$f = \frac{{\sigma_{\mathrm{max}}}^2}{2\epsilon\kappa}\left[|(\bar{\sigma}_-)^2 - (\bar{\sigma}_+)^2| + \beta(\bar{\sigma}_+ \ln\bar{\sigma}_+ + (1-\bar{\sigma}_+)\ln(1-\bar{\sigma}_+))\right] \ . \text{(linearized approximation)}$$

Nardi *et al.* pointed out that this function has an inflection point, giving a region of instability (Fig. 2*b*), when $\beta < 1/2$. According to (3.14), this means that either the maximum charge density e/a_0 must be large, or else the salt concentration $\hat{n}$ very small. Substituting some typical values for the charge per headgroup $a_0 = 0.5\,\mathrm{nm}$ and salt concentration $\hat{n} = 1\,\mathrm{mM} = 0.0006\,\mathrm{nm}^{-3}$ gives $\beta = 0.006$, well into the regime of instability.

Though we have found an instability, two remarks limit its interest. First, we have insisted that $0 < \sigma_+ < \sigma_{\mathrm{max}}$, so of course the charge densities $\sigma_+^{(a)}$ and $\sigma_+^{(n)}$ on our two zones are both positive: both zones are adhesive, unlike the experimental phenomenon we are trying to explain.

Moreover, we found no instability at all unless the charge density σ_{max} is quite large (recall also that $|\sigma_-|$ is assumed to be even greater than this). But at such large charges our linearized approximation breaks down! Our calculation becomes inconsistent just as it gets interesting. Much of this paper is dedicated to correcting this deficiency. We ask the reader to suspend disbelief momentarily while we implement the physical picture sketched in Sect. II in the linearized theory, where the formulæ are simple. Our claim is that the physical picture is robust and holds beyond this inadequate mathematical framework; we will support this claim by improving the calculation in Sect. IV–V.

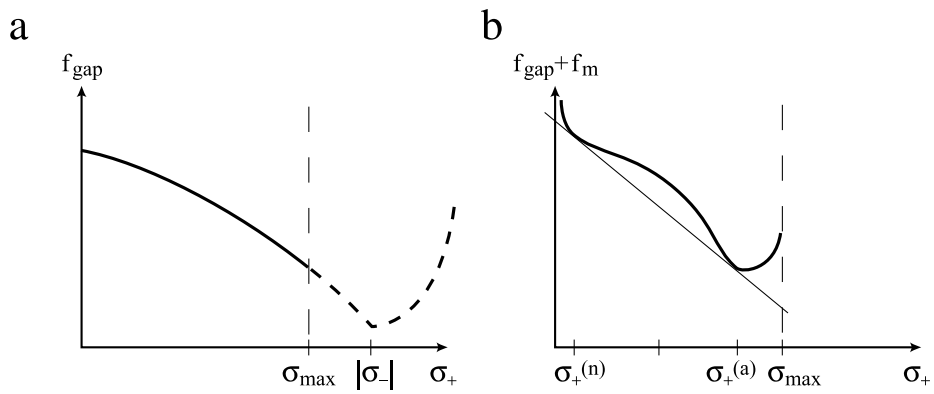

FIG. 2. *(a)* Sketch of the electrostatic part of the free energy ($f_{\rm gap}$, formula (3.10)), for a thick, mixed, membrane approaching a dielectric. We show the case where $|\sigma_-| > \sigma_{\rm max}$.
(b) Sketch of the total free energy ($f_{\rm gap}+f_{\rm m}$, including formula (3.12)), illustrating the Maxwell construction. The features of the curve have been exaggerated for clarity. The membrane will partition into a highly attractive region with charge density $\sigma_+^{(a)}$ and a somewhat-attractive region with $\sigma_+^{(n)}$.

D. Thin, permeable membrane

The previous subsection found that a highly-charged, thick, membrane can partition into a zone of strong adhesion and a second zone of weaker adhesion. In this subsection we will introduce another element of realism by accounting for the interior charges in the vesicle. To highlight the key role of the membrane as a barrier to counterions, we will first study the simpler case of a thin membrane *permeable* to ions, finding uniform attraction. This sets the stage for the more interesting case of an *im*permeable membrane in Sect. III E below.

Thus the new feature introduced in this subsection is that a membrane separates the world into two compartments, with electrolyte solution on each side (Fig. 3a). We continue to neglect the internal structure of the membrane, treating it as a single thin sheet of charge; in Sect. IV C below we will improve the analysis to include the bilayer structure and finite internal capacitance of real membranes.

To organize the calculation we first note that once again there is only one independent conserved quantity exchanged laterally between zones on the membrane, namely σ_+. Let

$$\sigma_{\rm in} \equiv \int_{-\infty}^{0} {\rm d}z\, e(n_+(z) - n_-(z)) \ . \tag{3.15}$$

be the areal density of mobile interior counterions. Note that unlike σ_+, which must be positive and less than $\sigma_{\rm max}$, the interior density $\sigma_{\rm in}$ can in principle have any sign and magnitude. We will hold $\sigma_{\rm in}$ fixed while optimizing over the gap spacing ℓ as in Sect. III B above. Since in this subsection we are assuming a permeable membrane, we then minimize over $\sigma_{\rm in}$ as well to obtain $f(\sigma_+)$. We will suppress explicit mention of the dependence on the dielectric charge σ_-, because σ_- is fixed.

The free energy density f can be regarded as an interior term from (3.8), plus a gap term, $f_{\rm gap}$ from (3.10), plus the membrane free energy $f_{\rm m}$ from (3.12). The interior term

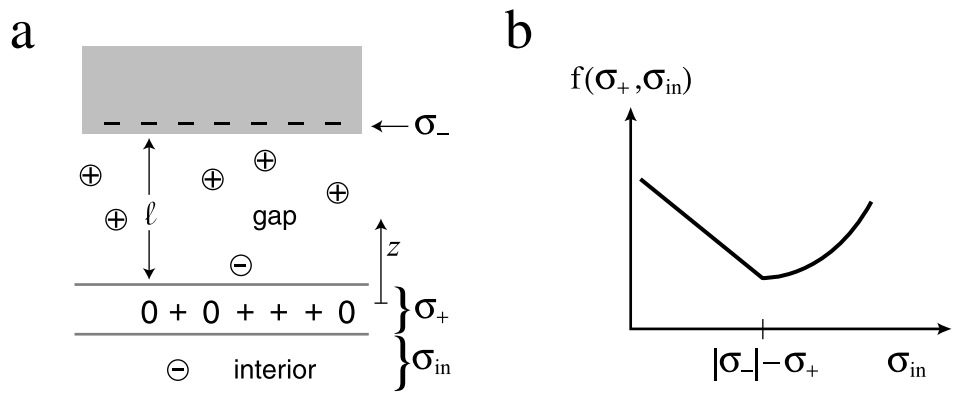

FIG. 3. *(a)* Schematic for the approach of a dielectric to a thin, permeable, membrane. Negative values of z in the text refer to the interior of the vesicle.

(b) Sketch of the free energy density $\bar{f}$ as a function of $\sigma_{\rm in}$, holding σ_+ fixed.

is $f_{\rm self}(-\sigma_{\rm in}) = (\sigma_{\rm in})^2/2\epsilon\kappa$. The gap sees opposing charge densities of σ_- and $(\sigma_+ + \sigma_{\rm in})$, so (3.10) gives $f_{\rm gap} = |\sigma_-{}^2 - (\sigma_+ + \sigma_{\rm in})^2|/2\epsilon\kappa$ and the equilibrium spacing is $\ell_*(\sigma_{\rm in}, \sigma_+) = \frac{1}{\kappa}\ln\frac{|\sigma_-|}{\sigma_+ + \sigma_{\rm in}}$.

The membrane free energy $f_{\rm m}$ is independent of $\sigma_{\rm in}$, so minimizing over $\sigma_{\rm in}$ gives (Fig. 3b) $\sigma_{{\rm in},*} = |\sigma_-| - \sigma_+$, a positive value corresponding to $\ell_* = 0$: the membrane comes into tight contact with the dielectric. Evaluating the free energy at this point gives

$$f(\sigma_+) = \frac{\sigma_{\rm max}{}^2}{2\epsilon\kappa}\left[(|\bar{\sigma}_-| - \bar{\sigma}_+)^2 + \beta\left(\bar{\sigma}_+\ln\bar{\sigma}_+ + (1-\bar{\sigma}_+)\ln(1-\bar{\sigma}_+)\right)\right] \ . \tag{3.16}$$

Computing the second derivative we see that this time every term of f is separately convex: there is no instability. Our result is physically reasonable. As the positive membrane approaches the dielectric, the latter's negative (minority) counterions and some of the positive (majority) counterions get released to the exterior. Since we have assumed the membrane is permeable, the remaining positive counterions pass through it, where many more pair up with interior negative ions from the membrane and get released to the interior. Since no counterions need to remain in the gap, we get tight contact between membrane and dielectric, which in effect become a single object of reduced charge density $\sigma_+ - |\sigma_-|$. The electrostatic self-energy of this composite object is a convex function, entropy never favors phase separation, and so there is no instability.

E. Thin, impermeable membrane

Previous subsections have shown that charge mobility alone can lead to an instability, but not to charge reversal (Sect. III C), and that introducing a coupled interior compartment alone does not even lead to instability (Sect. III D). Surprisingly, in this section and Sect. IV B below we will find that combining these two unpromising ingredients with the

hypothesis of a membrane impermeable to ions *can* lead to a charge-reversing instability.[6] The key observation is that an impermeable membrane has *two* conserved quantities independently exchanged between zones: the membrane charge $\bar{\sigma}_+$ and the interior counterion charge density $\bar{\sigma}_{\rm in}$.[7] In the previous subsection $\bar{\sigma}_{\rm in}$ could relax within a zone by passing through the membrane, and so we simply optimized f over it before applying the Maxwell construction. For an impermeable membrane we must instead apply the Maxwell construction to both $\bar{\sigma}_+$ and $\bar{\sigma}_{\rm in}$ jointly.

The geometry is the same as Fig. 3a. It will shorten some formulæ to define the total charge density

$$\bar{\sigma}_{\rm t} \equiv \bar{\sigma}_+ + \bar{\sigma}_{\rm in} \ . \tag{3.17}$$

The free energy density is the same as in Sect. III D, but this time we need a more general formulation than (3.16), since we are not simply evaluating at the optimal value of $\bar{\sigma}_{\rm in}$. In fact, there are three physically separate cases we must distinguish:
i) The membrane plus its trapped interior counterions may have greater charge density than the dielectric: $\bar{\sigma}_{\rm t} > |\bar{\sigma}_-|$.
ii) The membrane plus its trapped counterions may have lower charge density than the dielectric, but still be positive: $0 < \bar{\sigma}_{\rm t} < |\bar{\sigma}_-|$.
iii) The trapped counterions may overwhelm and effectively reverse the charge of the membrane: $\bar{\sigma}_{\rm t} < 0$. This is the charge-reversal we seek. In this case the equilibrium distance between the membrane and a negative dielectric is infinity; the membrane actually repels incoming negative objects.

The total free energy density in each of these cases (and still in the linearized approximation) now reads

$$\begin{aligned} f(\bar{\sigma}_+, \bar{\sigma}_{\rm t}) = \frac{{\sigma_{\rm max}}^2}{2\kappa\epsilon}\Big[(\bar{\sigma}_{\rm t} - \bar{\sigma}_+)^2 + \left\{ \begin{array}{ll} |(\bar{\sigma}_{\rm t})^2 - (\bar{\sigma}_-)^2| & \text{if } \bar{\sigma}_{\rm t} > 0 \\ (\bar{\sigma}_{\rm t})^2 + (\bar{\sigma}_-)^2 & \text{if } \bar{\sigma}_{\rm t} < 0 \end{array} \right\} \\ + \beta(\bar{\sigma}_+ \ln \bar{\sigma}_+ + (1 - \bar{\sigma}_+) \ln(1 - \bar{\sigma}_+))\Big] \ . \quad \text{(linearized approximation)} \end{aligned} \tag{3.18}$$

The function f defines a surface over the $(\bar{\sigma}_+, \bar{\sigma}_{\rm t})$-plane. If this surface is everywhere convex-down then there is no instability. If not, then it may be possible to bring a straight line up to the surface from below, touching it at two points of tangency but lower than

---

[6] We need not assume the membrane to be impermeable to *water*; because the bulk salt concentration is assumed the same on both sides, there will be no net osmotic flow.

[7] A third exchanged quantity, the net counterion charge density *outside* the membrane, is then fixed by charge neutrality: $\sigma_0 = -(\sigma_1 + \sigma_+ + \sigma_-)$. Similarly the density of neutral surfactants in the membrane is not independent, being given by $(2/a_0) - (\sigma_+/e)$. The numbers of individual counterions of each species are *not*, however, conserved, since neutral $\pm$ pairs can be exchanged with large reservoirs (the bulk solution inside and outside the vesicle) without macroscopic charge separation.

the surface at some point $(\bar{\sigma}_{+,\mathrm{av}}, \bar{\sigma}_{\mathrm{t,av}})$ lying between those tangency points. In this case a homogeneous system with average composition $(\bar{\sigma}_{+,\mathrm{av}}, \bar{\sigma}_{\mathrm{t,av}})$ will be able to reduce its free energy by partitioning into zones whose compositions are given by the two points of tangency.

We will assume that initially, when the membrane vesicle was formed and no dielectric spheres were present, the ions were in equilibrium across the membrane, so that half of them got trapped inside: $\bar{\sigma}_{\mathrm{t,av}} = \frac{1}{2}\bar{\sigma}_{+,\mathrm{av}}$. We will also for illustration generally take the membrane composition to be half charged and half neutral surfactants, so that the mole fraction $\bar{\sigma}_{+,\mathrm{av}} = \frac{1}{2}$. Finally we assume the approaching dielectric to have greater charge density than the maximum possible value for the membrane. For illustration we take $\bar{\sigma}_- = -3/2$. Summarizing, we will consider the illustrative case

$$\bar{\sigma}_{+,\mathrm{av}} = \tfrac{1}{2} \ , \qquad \bar{\sigma}_{\mathrm{t,av}} = \tfrac{1}{2}\bar{\sigma}_{+,\mathrm{av}} \ , \qquad \bar{\sigma}_- = -3/2 \ . \qquad \text{(illustrative case)}$$

In general there may be many lines in the $(\bar{\sigma}_+, \bar{\sigma}_{\mathrm{t}})$-plane, all passing through the point $(\bar{\sigma}_{+,\mathrm{av}}, \frac{1}{2}\bar{\sigma}_{+,\mathrm{av}})$ and all exhibiting the instability. In this case we must examine all the lines and choose the one which gives the absolute minimum in free energy. To do this systematically, we label the lines by the real number p and write each parametrically as

$$(\bar{\sigma}_+, \bar{\sigma}_{\mathrm{t}}) = (s, \tfrac{1-p}{2}\bar{\sigma}_{+,\mathrm{av}} + \tfrac{p}{2}s) \ , \qquad 0 < s < 1 \ . \tag{3.19}$$

In principle one could now plot f from (3.18) along the family of lines defined by (3.19), find the points of tangency, optimize over p, and finally obtain the sought instability and the charge densities $\bar{\sigma}_{\mathrm{t}}^{(a)}$ and $\bar{\sigma}_{\mathrm{t}}^{(n)}$ in the two zones as points of tangency, as described in Sect. III C above. If one of these (conventionally $\bar{\sigma}_{\mathrm{t}}^{(n)}$) proves to be negative, then we conclude that the membrane exhibits a charge-reversal instability, as was to be shown. In fact these steps are now rather easy to complete. But we have already remarked that the linearized theory is not accurate in the regime of high charge densities of interest to us. Accordingly we will now improve our theory by solving the full nonlinear Poisson-Boltzmann equation, then carry out the steps just described.

IV. NONLINEAR POISSON–BOLTZMANN THEORY

A. Basic formulæ

We introduce the useful new variable

$$\zeta \equiv \mathrm{e}^{\kappa z} \ . \tag{4.1}$$

It will also be convenient to define another nondimensional form of the charge density by

$$\tilde{\sigma} \equiv \sigma\kappa/2\hat{n}e = 2\bar{\sigma}/\beta \ . \tag{4.2}$$

and a nondimensional form of the free energy density by

$$\bar{f} = \frac{\kappa}{\hat{n}k_{\mathrm{B}}T} f \ . \tag{4.3}$$

The general solution to the Poisson-Boltzmann equation can be written in terms of elliptic functions (see for example [13]). Fortunately, however, we need only the zero-pressure solutions, corresponding to two walls which are free to adopt their equilibrium spacing ℓ_*, and these solutions consist of elementary functions [14,6]:

$$\bar{\psi}_\pm = \pm 2 \ln \frac{\zeta + 1}{\zeta - 1} \ . \tag{4.4}$$

At $\zeta \to \infty$ we then have $\bar{\psi}_\pm \to \pm 4/\zeta = \pm 4 \mathrm{e}^{-\kappa z}$, precisely the weak-field solution we found in Sect. III A.

The Poisson-Boltzmann equation is second-order, and so its general solution has two integration constants. We have fixed one of these by restricting to the zero-pressure case. The other one enters (4.4) rather trivially, due to the translation invariance of the PB equation: in (4.4) we are free to shift z, or equivalently multiply ζ by an arbitrary constant, thus obtaining a one-parameter family of zero-pressure solutions. In practice we will use (4.4) in the unshifted forms given above, but select the region $\zeta_1 < \zeta < \zeta_2$ to enforce Gauss's law at each of the two charged surfaces.

For example, for an isolated surface of charge density $\sigma_+ > 0$ we choose the solution $\bar{\psi}_+$ with one limit at infinity and the other at ζ_+, which we choose by requiring

$$\frac{\sigma_+}{\epsilon} = -\frac{k_\mathrm{B} T}{e} \frac{\mathrm{d}}{\mathrm{d}z} \bar{\psi}_+ \Big|_{z_+} \ .$$

or

$$\zeta_+ = \frac{2}{\tilde{\sigma}_+} \left(1 + \sqrt{1 + \tilde{\sigma}_+^2 / 4} \right) \ . \tag{4.5}$$

The free energy formula analogous to (3.8) is then obtained by substituting (4.4) into (3.5), to get

$$\bar{f}_\mathrm{self} = \frac{-8 \left(2 - \zeta_+ \ln(\frac{1+\zeta_+}{-1+\zeta_+}) \right)}{-1 + {\zeta_+}^2} + 2 \tilde{\sigma}_+ \ln \frac{\zeta_+ + 1}{\zeta_+ - 1} \qquad \text{(nonlinear theory)} \ . \tag{4.6}$$

Two surfaces of the same sign charge will repel to infinite separation, so we use this formula for each one separately. For a negatively-charged surface we simply replace $\tilde{\sigma}_+$ by $|\tilde{\sigma}_-|$ in (4.5).

It is instructive to compare (4.6) to the corresponding formula in the linearized approximation, formula (3.8) (Fig. 4). While the two formulæ agree at low charge density, the linearized formula overestimates the free energy by almost an order of magnitude at the high charge densities of interest to us. The nonlinear PB equation also predicts a narrower cloud of counterions than the linearized approximation at any given charge density.

For two oppositely charged surfaces at their equilibrium spacing we can generalize the argument given in Sect. III B above, again obtaining (3.10). Again suppose first that $\sigma_+ < |\sigma_-|$, and so $\zeta_+ > \zeta_-$. By the same logic as in Sect. III B, the potential $\bar{\psi}$ in the gap is just the same as that of an isolated surface of charge density σ_-, but truncated at some finite ζ_+.

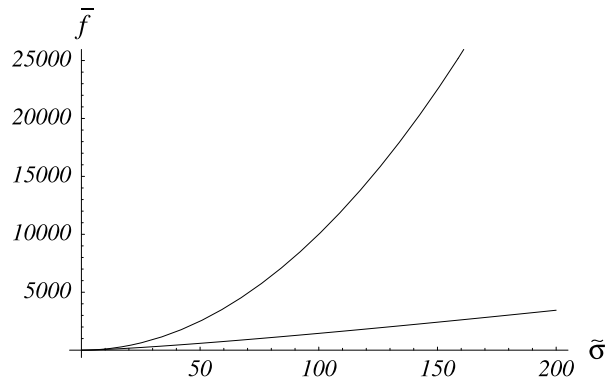

FIG. 4. The self-energy density of a charged surface $\bar{f}_{\rm self} = \kappa f_{\rm self}/k_{\rm B}T\hat{n}$ as a function of the dimensionless charge density $\tilde{\sigma}$. Top curve: Linearized approximation, eqn. (3.8). Bottom curve: Poisson-Boltzmann solution, eqn. (4.6). $f_{\rm self}$ is positive in our conventions; see Sect. III A.

Let us abbreviate the local integrand in (3.5) by $\Phi = \bar{\psi}\sinh\bar{\psi} - 2\cosh\bar{\psi} + 2$. This is the same for either of the two solutions $\bar{\psi}_\pm$. We thus get

$$\bar{f}_{\rm self}(\sigma_\pm) = \pm\frac{\kappa\sigma_\pm}{2e\hat{n}}\bar{\psi}_+(\zeta_\pm) + \int_{\zeta_\pm}^{\infty} {\rm d}\zeta\, \Phi$$

and

$$\bar{f}_{\rm gap}(\sigma_+,\sigma_-) = \frac{\kappa}{2e\hat{n}}(\sigma_-\bar{\psi}(\zeta_-) + \sigma_+\bar{\psi}(\zeta_+)) + \int_{\zeta_-}^{\zeta_+} {\rm d}\zeta\ \Phi\ .$$

But the last expression just equals $\bar{f}_{\rm self}(\sigma_-) - \bar{f}_{\rm self}(\sigma_+)$. Repeating for the opposite case $\sigma_+ > |\sigma_-|$, we get the desired combination formula (3.10).

B. Thin, impermeable membrane

Proceeding now as in Sect. III E, we combine (4.2), (4.3), (4.5), (4.6), (3.10), (3.12), and (3.14) to obtain the analog of the linearized formula (3.18): the nondimensional free energy density of the membrane+dielectric system at its equilibrium spacing ℓ_*, as a function of the local membrane charge density σ_+ and the net charge density $\sigma_{\rm t}$ of counterions trapped inside the membrane vesicle, is now

$$\bar{f}(\bar{\sigma}_+,\bar{\sigma}_{\rm t}) = \bar{f}_{\rm self}(\bar{\sigma}_{\rm t} - \bar{\sigma}_+) + \left\{ \begin{array}{ll} |\bar{f}_{\rm self}(\bar{\sigma}_{\rm t}) - \bar{f}_{\rm self}(\bar{\sigma}_-)| & \text{if } \bar{\sigma}_{\rm t} > 0 \\ \bar{f}_{\rm self}(\bar{\sigma}_{\rm t}) + \bar{f}_{\rm self}(\bar{\sigma}_-) & \text{if } \bar{\sigma}_{\rm t} < 0 \end{array} \right\}$$
$$+ \frac{4}{\beta}(\bar{\sigma}_+\ln\bar{\sigma}_+ + (1-\bar{\sigma}_+)\ln(1-\bar{\sigma}_+))\ . \qquad (4.7)$$

Here $\bar{\sigma}_{\rm t} = \bar{\sigma}_+ + \bar{\sigma}_{\rm in}$ as before and $\bar{f}_{\rm self}(\bar{\sigma})$ is the function defined by (4.5), (4.6) evaluated at $\tilde{\sigma} = 2\bar{\sigma}/\beta$. Thus at low charge densities the first two terms of (4.7) contain factors of $1/\beta^2$, and so dominate the last (mixing-entropy) term, just as in (3.18).

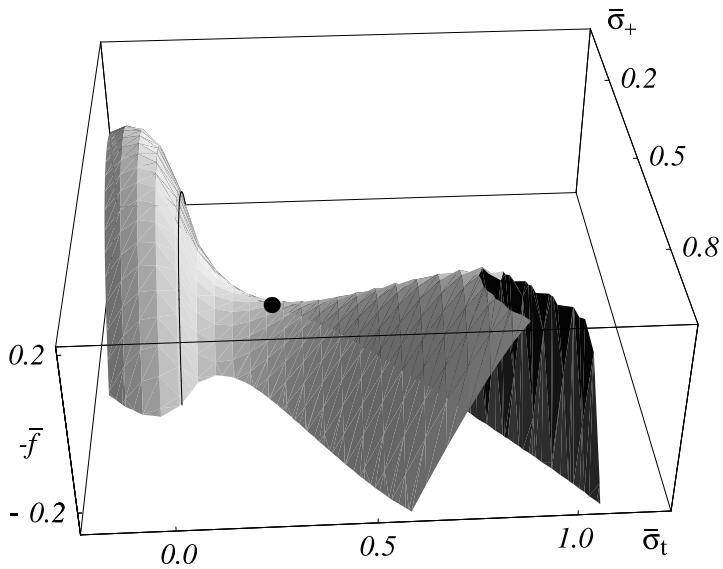

FIG. 5. Free energy density $\bar{f}(\bar{\sigma}_+, \bar{\sigma}_t)$ for a thin, impermeable, membrane. For easier visualization we have inverted the figure, rescaled, and added a linear function, plotting $-\bar{f}(\bar{\sigma}_+, \bar{\sigma}_t)/1000 + 218.0 + 6.0\bar{\sigma}_+ - 11.4\bar{\sigma}_t$ instead of f. The solid curve is the locus of points where $\bar{\sigma}_t = 0$; points to the left of this curve represent charge-reversed states. The heavy dot is the point $(\bar{\sigma}_{+,\mathrm{av}}, \bar{\sigma}_{t,\mathrm{av}}) = (1/2, 1/4)$ representing the average membrane composition chosen for our illustrative calculation. The two hills in the graph imply, *via* the Maxwell construction, that the system's ground state consists of two coexisting zones. Since furthermore the hills straddle the solid curve, one of the zones is charge-reversed. [Adapted by permission from [4]. © 1999 American Association for the Advancement of Science.]

We can now carry out the program outlined in Sect. III E for the illustrative parameter values $\hat{n} = 1\,\mathrm{mM}$, $a_0 = 0.5\,\mathrm{nm}^2$, $\beta = 0.006$, $\bar{\sigma}_- = -3/2$, and $\bar{\sigma}_{+,\mathrm{av}} = 1/2$ discussed earlier. Fig. 5 shows the surface defined by (4.7). For clarity we have shown $-\bar{f}$ instead of $\bar{f}$, so that thermodynamic stability would correspond to an inverted bowl shape. We have also tilted the graph by adding a convenient linear function to $-\bar{f}$, to highlight the saddle shape. The linear function was selected by trial and error. Adding it does not change the points of tangency between the surface and a straight line.

The graph clearly displays the instability we were seeking. Moreover, one of the two hills on the surface clearly lies to the left of the line of charge reversal, $\{\bar{\sigma}_t = 0\}$. To make this qualitative observation precise, we must now evaluate (4.7) along the family of lines specified by (3.19), perform the Maxwell construction on each line, and choose the value of p whose tangent line has the lowest value of $\bar{f}$ at the point $\bar{\sigma}_{+,\mathrm{av}}$. Fig. 6 shows the result of this analysis for the illustrative values $p = 2.4$ and 3.8, and the optimal value $p = 2.9$.

The figure shows coexistence between a zone with $\bar{\sigma}_+^{(a)} = 0.95$, and another zone with $\bar{\sigma}_+^{(n)} = 0.25$. The latter zone thus presents total charge density $\bar{\sigma}_t = -0.11$ to the outside of the vesicle. Since this is negative, this zone is charge-reversed and deserves its name

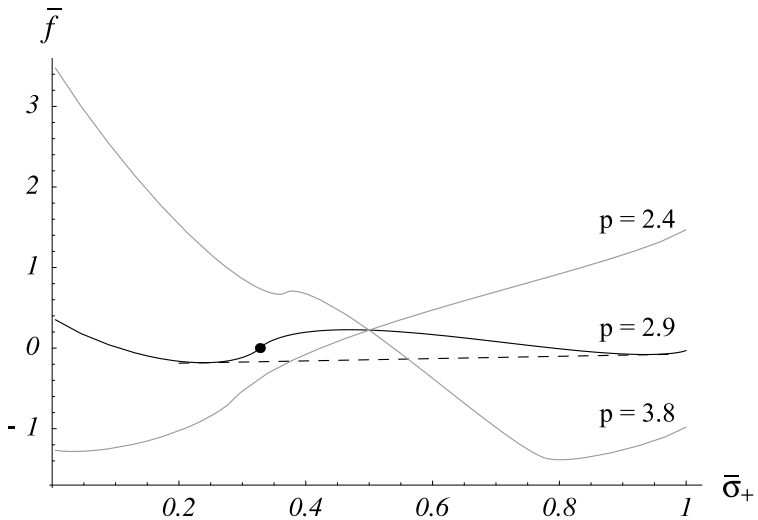

FIG. 6. Three slices through Fig. 5 along lines passing through the average-composition point $(\bar{\sigma}_+, \bar{\sigma}_{\rm t}) = (1/2, 1/4)$. The total charge density seen from outside the membrane is taken to be $\bar{\sigma}_{\rm t} = ((1-p)\bar{\sigma}_{+,\rm av} + p\bar{\sigma}_+)/2$ for various values of p. Unlike Fig. 5 we have not inverted this graph. Two illustrative slices (gray curves) show $p = 2.4$ and 3.8. The black curve, with $p = 2.9$, gives the most advantageous mixed state, since its tangent line intersects $\bar{\sigma}_+ = \bar{\sigma}_{+,\rm av} = 1/2$ at the lowest value of $\bar{f}$; hence $p_* \approx 2.9$. The dashed line shows coexistence between an adhesion zone with $\bar{\sigma}_+^{(a)} = 0.95$, covering a fraction $\gamma_* = 0.36$ of the vesicle, and a nonadhesive zone with $\bar{\sigma}_+^{(n)} = 0.25$. The heavy dot shows the point of charge reversal, where $\bar{\sigma}_{\rm t} = 0$. Since the points of tangency lie on opposite sides of this dot, the nonadhesive zone indeed presents net negative charge to the outside world. Again the curves have been tilted for viewing by plotting $\bar{f}/1000 + 10.9\bar{\sigma}_+ - 15.2$.

as a "nonadhesive" zone. Indeed the effect is large: $\bar{\sigma}_{\rm t}$ is -45% as great as the charge $\bar{\sigma}_{+,\rm av}/2 = 1/4$ presented to the outside world when there are no adhering dielectrics spheres. Recalling that $\gamma\bar{\sigma}_+^{(a)} + (1-\gamma)\bar{\sigma}_+^{(n)} = \bar{\sigma}_{+,\rm av}$, we find that the adhesion zone covers 36% of the vesicle. These results were announced in [4].

C. Finite thickness, bilayer membrane

While the above results are encouraging, and show the mathematical possibility of a charge-reversal instability, our model needs considerable refinement before we can take its results seriously. In this subsection we begin this task by acknowledging the bilayer character of the membrane and its finite capacitance, both neglected up to this point. The results in this section were also announced in [4].

Instead of idealizing the membrane as a thin sheet of charge density σ_+, we now regard it as two sheets of charge density $u\sigma_+$ and $(1-u)\sigma_+$ representing the charged headgroups of the inner and outer surfactant layers respectively (see Fig. 1d). These two layers of charge are

separated by a dielectric layer of thickness t and dielectric constant $\epsilon_{\rm m}$, creating a capacitor of capacitance $c = \epsilon_{\rm m}/t$ per area. We will estimate c using the value 0.01 pF/μm^2 typical for artificial bilayer membranes [15] and make the useful abbreviation

$$\tau \equiv t\kappa\epsilon/\epsilon_{\rm m} = \kappa\epsilon/c \ . \tag{4.8}$$

Then $\tau \approx 7$ at salt concentration $\hat{n} = 1\,$mM, or more generally $\tau \approx 7\sqrt{\hat{n}/{\rm mM}}$.

The free energy formula (4.7) used in Sect. IV B needs only two simple modifications: 1) Since the membrane still presents charge density $\sigma_+ - \sigma_{\rm t}$ to the interior solution and $\sigma_{\rm t}$ to the exterior (Fig. 1), the terms involving $\bar{f}_{\rm self}$ are unchanged. Now, however, when $\sigma_{\rm in} + u\sigma_+$ is nonzero (or equivalently $\sigma_{\rm t} + (u-1)\sigma_+ \neq 0$), there will be a nonzero electric field in the membrane's interior, with a capacitive energy cost per area of $(\sigma_{\rm t} + (u-1)\sigma_+)^2/2c$.
2) The membrane now consists of *two* fluid monolayers of mixed charged and neutral surfactants. Each monolayer has a maximal density $\frac{1}{2}\sigma_{\rm max} = e/a_0$, attained when the density of neutrals is zero. Accordingly we replace the mixing entropy $f_{\rm m}$ from (3.12) by

$$\frac{k_{\rm B}T}{a_0}\left[\frac{u\sigma_+}{\sigma_{\rm max}/2}\ln\frac{u\sigma_+}{\sigma_{\rm max}/2} + \cdots\right] \ .$$

Casting everything into the nondimensional forms defined above, we see that we must add to the formula (4.7) for $\bar{f}$ the expression

$$\begin{aligned}\frac{4\tau}{\beta^2}(\bar{\sigma}_{\rm t} + (u-1)\bar{\sigma}_+)^2 + \frac{2}{\beta}\Big[&2u\bar{\sigma}_+\ln(2u\bar{\sigma}_+) + (1-2u\bar{\sigma}_+)\ln(1-2u\bar{\sigma}_+) \\ &+2(1-u)\bar{\sigma}_+\ln 2(1-u)\bar{\sigma}_+ + (1-2(1-u)\bar{\sigma}_+)\ln(1-2(1-u)\bar{\sigma}_+)\Big].\end{aligned} \tag{4.9}$$

To use our formulæ we add (4.9) to (4.7) and again hold fixed the two conserved quantities $\bar{\sigma}_+$ and $\bar{\sigma}_{\rm t}$. As before we must optimize over all other variables, in this case just u, before performing the Maxwell construction as in Sect. IV B. We can simply optimize (4.9) over u, since u does not enter (4.7). However, this optimization is subject to the four inequalities which u must obey:

$$0 < u\bar{\sigma}_+ < 1/2 \ , \quad 0 < (1-u)\bar{\sigma}_+ < 1/2 \ .$$

A graphical analysis similar to the one shown in Fig. 6 now gives (Fig. 7) that the best line through $(\bar{\sigma}_+, \bar{\sigma}_{\rm t}) = (1/2, 1/4)$ has $p \approx 2$ (see (3.19)), with points of tangency at $\bar{\sigma}_+^{(a)} = 0.247$, and $\bar{\sigma}_+^{(n)} = 0.65$. Proceeding as in Sect. IV B gives coverage $\gamma_* = 63\%$ at equilibrium and $\bar{\sigma}_{\rm t} = -0.003$, or about -1.2% of the charge density presented to the outside world when no dielectric spheres are present.

We can readily understand the qualitative features of these results. Since τ is large, electric fields inside the membrane are energetically costly and the two sides of the membrane are nearly independent. Thus the interior ion charge density $\sigma_{\rm in}$ remains nearly uniform, and hence nearly equal to $-\sigma_{+,{\rm av}}/2$, and similarly the inner monolayer charge density $u\sigma_+ \approx \sigma_{+,{\rm av}}/2$. Then the total charge density $\bar{\sigma}_{\rm t} \approx (1-u)\bar{\sigma}_+ \approx \frac{1-u}{2u}\bar{\sigma}_{+,{\rm av}}$ (see Fig. 1*d*), and (3.19) requires that either $u = 1/2$ or $p \approx 2$. The solution $u = 1/2$ is unphysical; the solution $p \approx 2$ is just what we found numerically. To reverse its charge, the membrane must allow electric

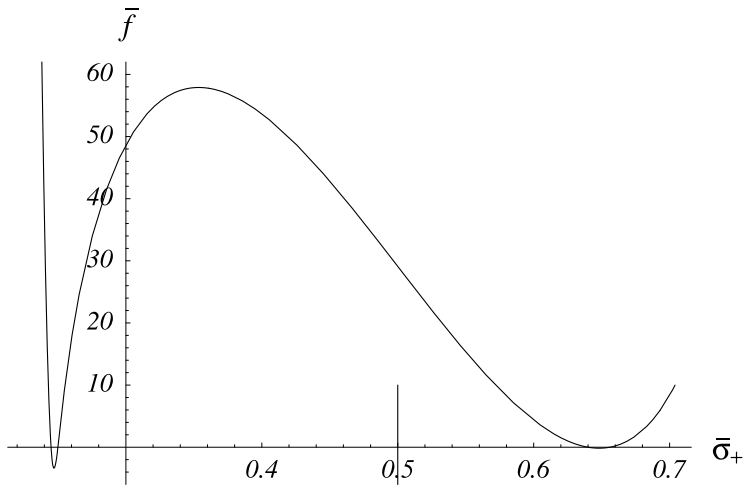

FIG. 7. Free energy density along the optimal line $p \approx 2$ for a finite-thickness, bilayer membrane. The long tick on the abscissa is at $\bar{\sigma}_{+,\mathrm{av}}$, the illustrative value for average bilayer concentration studied in the text. The point of charge reversal is $\bar{\sigma}_+ = 0.25$, which is the second point from the left where the graph intercepts the abscissa. Since the tangent point is slightly to the left of this, at $\bar{\sigma}_+^{(n)} = 0.247$, we again find a slight charge reversal. Again the graph has been scaled and shifted to bring out its structure: we have plotted the quantity $\bar{f} - 12750 + 5615\bar{\sigma}_+$.

fields in its interior (see Fig. 1*d*); the high cost of doing this accounts for the very sharp left-hand dip in Fig. 7 compared to Fig. 6, and for the greatly reduced degree of charge reversal in the finite-thickness case. The charge-reversal effect diminishes for larger values of τ, as we predicted in Sect. II. According to (4.8) this means the effect will disappear either for thick membranes or at large enough ion strength $\hat{n}$. Numerically we find the critical value to be about 20 mM, roughly as seen in the experiments of [4,5].

Though the charge-reversal effect seems small, it is enough to cause the rejection of additional negative dielectric spheres. To estimate the magnitude of this effect, consider what is needed to increase γ from its equilibrium value γ_* to $\gamma_* + \delta$. To do this we must choose new values of $\bar{\sigma}_+^{(a)} + \epsilon^{(a)}$ and $\bar{\sigma}_+^{(n)} + \epsilon^{(n)}$, subject to the condition (3.13), which now reads

$$(\gamma_* + \delta)(\bar{\sigma}_+^{(a)} + \epsilon^{(a)}) + (1 - \gamma_* - \delta)(\bar{\sigma}_+^{(n)} + \epsilon^{(n)}) = \bar{\sigma}_{+,\mathrm{av}} \ .$$

We then minimize the total free energy F over $\epsilon^{(a)}$ and $\epsilon^{(n)}$ subject to this constraint, finding that the increase in F when we force a nonequilibrium value of γ is

$$\Delta F = \frac{k_{\mathrm{B}} T \hat{n}}{\kappa} \frac{1}{2} (\bar{\sigma}_+^{(a)} - \bar{\sigma}_+^{(n)})^2 \left[\frac{1 - \gamma_*}{\bar{f}''_{(n)}} + \frac{\gamma_*}{\bar{f}''_{(a)}} \right]^{-1} A\delta^2 \ .$$

In this expression $\bar{f}''_{(a)}$ denotes $\frac{\mathrm{d}^2 \bar{f}}{\mathrm{d}\bar{\sigma}_+^2}\Big|_{\bar{\sigma}_+^{(a)}}$, *etc.*, and A is the total membrane area. Bringing an additional $1\,\mu\mathrm{m}^2$ of negative dielectric into contact with a vesicle of area $4\pi(10\,\mu\mathrm{m})^2$ gives

$\delta = 0.00083$. Evaluating numerically then gives $\Delta F \approx 3000 k_{\rm B}T$, a huge barrier to adhesion, and similarly if we pull away $1\,\mu{\rm m}^2$ of adhering dielectric.

V. EFFECTS OF ION CORRELATIONS

The charge density near a highly-charged surface can become so great as to invalidate the mean-field theory we have used so far. The resulting changes in the force between two plates have been the object of intense study since the discovery that the total force can become attractive for two *like*-charged plates, in the presence of multivalent counterions [16,17]. The situation we will need to study will be much simpler than that one, for two reasons. First, we are only interested in the free energy density at *zero* force (*i.e.*, equilibrium). Secondly, our effect has arisen already at the level of mean-field theory. Since we consider the case of *mono*valent counterions only, *i.e.* in the regimes of small to moderate ion interactions, correlation effects will turn out to be a modest correction to the main, mean-field, contribution. Thus we are in the regime opposite to that recently studied in refs. [18,19].

The criterion for mean-field theory to be valid is roughly that the electrostatic potential energy of two ions at the mean ionic separation be smaller than the thermal energy: $e^2 n_\pm^{1/3}/4\pi\epsilon < k_{\rm B}T$, or equivalently that $n_\pm \ell_B^3 < 1$. Any isolated surface, no matter how highly charged, will have a distance beyond which this criterion is satisfied, and so our universal Poisson-Boltzmann solution (4.4) will be valid there. We will call the boundary of this region $z = z_s$. We find z_s using (4.4) and (3.4), obtaining $z_s = 0.28\,{\rm nm}$ for our illustrative case of ambient salt concentration $\hat{n} = 1\,{\rm mM}$.

Thus any isolated planar surface has exactly the same potential (equation (4.4)) as any other, for $z > z_s$. The charge density σ_+ enters only *via* the location z_+ of the surface in the coordinate z. Given a surface of charge density σ_+, we compute $z_+ = \kappa^{-1}\ln\zeta_+$, where ζ_+ is given by (4.5). If $z_+ > z_s = 0.28\,{\rm nm}$, then mean-field theory is everywhere accurate and there is no correlated-ion cloud near the surface. In the opposite case, that part of the ion cloud lying within the layer $z_+ < z < z_s$ will have nonnegligible correlations. Since z_+ is always positive, this layer is never any thicker than a typical ion radius, and so may be treated as a two-dimensional classical charged gas [20]. This approach may be regarded as an approximation to other, more refined, calculations (*e.g.* refs. [21,22]).

The effect of correlations will be to reduce the free energy density, as ions can avoid each other, reducing their electrostatic self-energy. To apply the results of Totsuji, originally derived for use in the study of electrons adsorbed onto liquid helium [20], we need to know the two-dimensional density m of counterions in the correlated layer. m simply equals σ_+/e minus the total density in the uncorrelated region $z > z_s$. Again using (4.4) and (3.4) in the latter region, we find $m = (\sigma_+/e) - 0.81\,{\rm nm}^{-2}$. If this quantity is negative then there simply is no correlated layer and $m = 0$. Defining the plasma parameter as $\Gamma = \ell_B\sqrt{\pi m}$, the correlation energy density can then be represented by the interpolation formula $E_c = mk_{\rm B}T\Gamma(-1.07 + \frac{1}{2.2\Gamma+1.3})$, which is approximately valid over the range $0 < \Gamma < 5000$ [20]. Fig. 8 shows the resulting change in the free energy density, obtained from the thermodynamic formula $f_c(m) = mk_{\rm B}T\int_0^\Gamma \frac{{\rm d}\Gamma}{\Gamma}\frac{E_c}{mk_{\rm B}T}$ for the correlation contribution f_c to the free energy density.

When two oppositely-charged surfaces face each other, we have seen how the minority

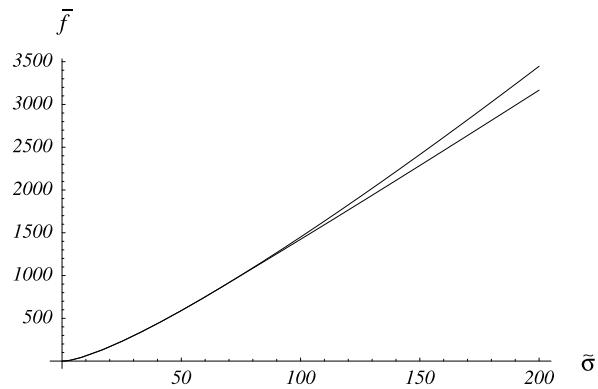

FIG. 8. Correction to the self-energy density $\bar{f}_{\rm self}$ from counterion correlations. The upper curve is the Poisson–Boltzmann result (lower curve of Fig. 4); the lower curve includes the correction f_c discussed in the text.

surface will be stripped of its counterions; the majority surface may, however, have a correlated ion cloud, so we add $f_c(m)$ to its free energy density. Since in the situations of interest to us the majority surface is always the dielectric sphere, and since m depends only on the surface's charge (not on the presence of the other surface), we find that *the correlation correction to the free energy of the negatively-charged dielectric surface is a constant*, and may simply be dropped. We do need to include the correlation free energy of the membrane's interior surface, but for a finite-thickness membrane this too is nearly a constant, since as we have seen the inner monolayer's charge density $u\sigma_+$ deviates only slightly from $\sigma_{+,\rm av}/2$. Finally, in conditions of charge reversal the *outer* monolayer becomes isolated and can have an ion cloud of its own. Since as we have seen the degree of charge reversal is very small, the density m of this last ion cloud is very small and the correlation contribution is negligible.

We have just outlined qualitatively why counterion correlations may be expected to have little effect on the results given in Sect. IV C. Indeed, the numerically calculated graph analogous to Fig. 7 is not appreciably different from that graph, and we do not display it here.

VI. DISCUSSION

We have proposed a theoretical explanation for the phenomenon of electrostatic adhesion saturation observed experimentally in [4,5]. While the experimental system has not been systematically explored yet, our model reproduces qualitatively the surprising the phenomenon of charge reversal and several salient experimental facts [4,5]:
1) Adhesion saturation occurs only with *mixed* bilayer vesicles, that is, at mole ratios $\bar{\sigma}_{+,\rm av}$ not too close to zero or unity.
2) It occurs only under conditions of sufficiently low salt.
3) The saturated state has a very definite number of adhering objects (γ_* is fixed for each vesicle).

Our analysis has omitted many familiar colloidal-force effects. Many of these are short-ranged (*e.g.* solvation forces), weak compared to electrostatic forces (*e.g.* undulation repulsion), or rapidly decreasing with distance (*e.g.* van der Waals forces). In addition we have neglected all finite ion-size effects. We believe that our conclusions will be robust when such effects are introduced, in part because the crucial physics of charge reversal involves the immediate neighborhood of the left-hand dip in Fig. 7, namely, the separation between the charge-reversal point and the tangency point. But the distance ℓ_* between the membrane and dielectric diverges as we approach the charge-reversal point from the right, so this physics is controlled by the long-distance behavior of the forces. Certainly the exact location of the tangent point depends on the right-hand part of Fig. 7 as well, where our theory is not reliable. But this dependence is small due to the sharpness of the left-hand dip in the free energy density. Even if the right-hand side of the graph differs from what we computed, there should be a range of membrane compositions $\bar{\sigma}_{+,\mathrm{av}}$ greater than $\bar{\sigma}_+^{(n)}$ but low enough to be in the left part of the graph, and hence yielding the sort of zone separation we have studied.

We have examined only *equilibrium* states. It is quite possible that the experimental system of [4,5] is not in equilibrium, *i.e.* that the observed coverage γ is less than the equilibrium value γ_* because the last one or two balls is initially repelled by a finite free-energy barrier. But our goal was to understand the surprising existence of *any* barrier, not to predict a specific value for γ_*, which in any case depends on the membrane composition.[8]

The analysis suggests a number of experimental tests of our mechanism. A mixed vesicle adhering to a charged dielectric surface [9] may provide a more controlled geometry than that of [5]; in this case adhesion saturation suggests the possibility of observing an adhering, yet flaccid, vesicle. A more ambitious test could be arranged by washing out the exterior solution, replacing it by another of different ion strength but the same osmolarity, while pinning a single vesicle for observation with a micropipette. Our formulæ generalize readily to the case where the ionic strength $\hat{n}$ is different inside and outside the vesicle. In this way may be possible reversibly to turn adhesion saturation on and off.

ACKNOWLEDGMENTS

We thank R. Bruinsma, I. Rouzina, and B. Shklovskii for discussions, and especially H. Aranda-Espinoza, N. Dan, T. C. Lubensky, L. Ramos, and D. A. Weitz for an earlier collaboration leading to the ideas presented here. This work was supported in part by NSF grant DMR98-07156.

---

[8]Moreover, the observed ball coverage does not directly give γ, since the degree of each ball's coverage is not optically observable; see [5].

APPENDIX: NOTATION

Constants

We work in SI units. Thus the potential around a point charge q in vacuum is $\psi(r) = q/4\pi\epsilon_0 r$, where $\epsilon_0 = 9 \cdot 10^{-12}$ Farad/meter. We treat water as a continuum dielectric with $\epsilon = 80\epsilon_0$; inside the membrane $\epsilon_m \approx 2\epsilon_0$. The Bjerrum length in water is $\ell_B = e^2/4\pi\epsilon k_{\rm B}T$; thus $4\pi\ell_B = 8.7\,\mathrm{nm}$.

Parameters

We take for illustration a typical ambient salt concentration of $\hat{n} = 1\,\mathrm{mM}{=}6 \cdot 10^{-4}\,\mathrm{nm}^{-3}$. Then the inverse Debye length is $\kappa = \sqrt{2\hat{n}e^2/\epsilon k_{\rm B}T} = \sqrt{\hat{n}/\mathrm{mM}}/(9.8\,\mathrm{nm})$. The salt concentration inside the vesicle is the same, due to osmotic clamping.

We suppose a mixture of surfactants, which for simplicity have equal area per headgroup $a_0 = 0.5\,\mathrm{nm}^2$. Then $\sigma_{\rm max} = 2e/a_0$ is the maximum bilayer charge density and the parameter $\beta = 2\hat{n}a_0/\kappa = 0.006$ measures the relative importance of mixing-entropy and electrostatic effects.

We use a typical artificial bilayer capacitance of $c = 0.01\,\mathrm{pF}/\mu\mathrm{m}^2$, which enters only in combination with the membrane thickness t *via* $\tau = t\kappa\epsilon/\epsilon_{\rm m} \approx 7\sqrt{\hat{n}/\mathrm{mM}}$.

For illustration we take the experimentally-controllable mole fraction of charged surfactants to be $\bar{\sigma}_{+,\rm av} = 1/2$ and one half of the corresponding counterions to be trapped on the vesicle interior, so that $\bar{\sigma}_{\rm t,av} = \bar{\sigma}_{+,\rm av}/2 = 1/4$. We also take the approaching charged dielectric objects to have charge density 50% greater than the membrane, or $\bar{\sigma}_- = -3/2$.

Variables

We generally denote nondimensionalized quantities with a bar or tilde: thus $\bar{\sigma} \equiv \sigma/\sigma_{\rm max}$, while $\tilde{\sigma} = \sigma\kappa/2\hat{n}e = 2\bar{\sigma}/\beta$. Also the free energy density f gives rise to $\bar{f} = \kappa f/\hat{n}k_{\rm B}T = f/(6 \cdot 10^3 k_{\rm B}T/\mu\mathrm{m}^2)\sqrt{\hat{n}/\mathrm{mM}}$, while the electrostatic potential ψ gives $\bar{\psi} = e\psi/k_{\rm B}T$. Various contributions to f include the mixing entropy of membrane surfactants $f_{\rm m}$ and the correlation contribution f_c.

The charge density σ of a surface determines its Gouy-Chapman length $\lambda_{\rm GC} = 2\epsilon k_{\rm B}T/e\sigma$. Various charge densities in the text are defined in Fig. 1, for example $\sigma_t = \sigma_{\rm in} + \sigma_+$. m denotes the 2d *number* density of ions in the dense correlated cloud near a surface. m in turn determines the plasma parameter $\Gamma \equiv \ell_B\sqrt{\pi m}$.

Geometrical quantities include the gap width ℓ, the total membrane area A, the fraction γ of A in the adhesion zone and its equilibrium value γ_*. The distance z from a surface is sometimes expressed using $\zeta = \mathrm{e}^{\kappa z}$.

REFERENCES

[1] S. Hachisu, Y. Kobayashi, and A. Kose. *J. Colloid Interface Sci*, 42:342, 1973.

[2] R. Williams, R. S. Crandall, and P. J. Wojtowitz. *Phys. Rev. Lett.*, 37:348, 1976.

[3] A. D. Dinsmore, P. B. Warren, W. C. K. Poon, and A. G. Yodh. Fluid-solid transitions on walls in binary hard-sphere mixtures. *Europhys. Lett.*, 40:337–342, 1997.

[4] H. Aranda-Espinosa, Y. Chen, N. Dan, T. C. Lubensky, P. Nelson, L. Ramos, and D. A. Weitz. Electrostatic repulsion of positively charged vesicles and negatively charged objects. *Science*, 285:394–397, 1999.

[5] L. Ramos, T. C. Lubensky, N. Dan, P. Nelson, and D. A. Weitz. Surfactant-mediated two-dimensional crystallization of colloidal crystals. *Science*, 286:2325–2328, 1999.

[6] W. B. Russel, D. A. Saville, and W. R. Schowalter. *Colloidal Dispersions*. Cambridge U. Press, New York, 1989.

[7] J. N. Israelachvili. *Intermolecular and surface forces*. Academic Press, London, 2nd edition, 1991.

[8] S. A. Safran. *Statistical thermodynamics of surfaces, interfaces, and membranes*. Addison-Wesley, Reading, MA, 1994.

[9] J. Nardi, R. Bruinsma, and E. Sackmann. Adhesion-induced reorganization of charged fluid membranes. *Phys. Rev.*, E58:6340–6354, 1998.

[10] V. A. Parsegian and D. Gingell. On the electrostatic interaction across a salt solution between two bodies bearing unequal charges. *Biophys. J.*, 12:1192–1204, 1972.

[11] J. Nardi, T. Feder, R. Bruinsma, and E. Sackmann. Adhesion-induced reorganization of charged fluid membranes: Phase separation and blistering. *Europhysics Letters*, 37:371, 1997. [Erratum ibid. 38 (1997) 159].

[12] L. D. Landau and E. M. Lifshitz. *Electrodynamics of continuous media*. Pergamon, Oxford, 2nd edition, 1984.

[13] S. H. Behrens and M. Borkovec. Exact Poisson-Boltzmann solution for the interaction of dissimilar charge-regulating surfaces. *Phys. Rev.*, E60:7040–7048, 1999.

[14] E. J. W. Vervey and J. Th. G. Overbeek. *Theory of the stability of lyophobic colloids*. Elsevier, New York, 1948.

[15] R. B. Gennis. *Biomembranes*. Springer, New York, 1989.

[16] L. Guldbrand, B. Jönnson, H. Wennerström, and P. Linse. Electrical double layer forces. A Monte Carlo study. *J. Chem. Phys.*, 80:2221–2228, 1984.

[17] R. Kjellander and S. Marcelja. *Chem. Phys. Lett.*, 112:49, 1984.

[18] I. Rouzina and V. A. Bloomfield. Macroion attraction due to electrostatic correlation between screening counterions. *J. Phys. Chem.*, 100:9977–9989, 1996.

[19] V. I. Perel and B. I. Shklovskii. Screening of a macroion by multivalent ions: a new boundary condition for the Poisson-Boltzmann equation and charge inversion. *Physica*, A274:446–453, 1999.

[20] H. Totsuji. Numerical experiments on two-dimensional electron liquids. *Phys. Rev.*, A17:399–406, 1978. Totsuji assumed a passive, uniform neutralizing background, and only one species of mobile charge. We justify the use of this idealization in our system by noting that at high charge densities the concentration of ions with the same sign as the surface is negligible, and the compressibility of the 2d liquid of charged surfactants is much lower than that of the counterions, since the former are nearly tightly packed at area fraction nearly unity. At low charge densities the correlation correction is in any case negligible.

[21] R. Kjellander. *Ber. Bunsenges. Phys. Chem.*, 100:894, 1996.

[22] P. Attard, D. J. Mitchell, and B. W. Ninham. Beyond Poisson-Boltzmann: Images and correlations in the electric double layer. I. Counterions only. *J. Chem. Phys.*, 88:4987–96, 1988.